Proceedings of the XXXVIII International School and Conference on the Physics of Semiconductors "Jaszowiec" 2009

Magnetic Force Microscopy Study of $Zn_{1-x}Co_xO$ Nanowires Grown by Rapid Thermal Evaporation

M. Aleszkiewicz[a,b], K. Fronc[a], P. Aleszkiewicz[a], W. Zaleszczyk[a], P. Dziawa[a], T. Wojciechowski[a], T. Wojtowicz[a] and G. Karczewski[a]

[a]Institute of Physics, Polish Academy of Sciences, al. Lotników 32/46, 02-668 Warsaw, Poland

[b]Dept. Mathematics and Natural Sciences, College of Sciences, UKSW, Warsaw, Poland

In this work we studied domain structure of $Zn_{1-x}Co_xO$ nanowires which are single arms of tetrapode crystals. The as-grown material exhibits hysteretic behavior even at room temperature as revealed by SQUID mesurements. In order to get insight into the magnetic properties of individual tetrapodes they were dismembered into nanowires of nanometric diameters, deposited on a flat substrate and imaged by magnetic force microscopy. A magnetic interaction between the magnetic force microscopy probe and single nanowires has been detected which confirms that nanometric volume of the material possesses a magnetic moment. The magnetic force microscopy contrast is attractively independent of the tip magnetization direction which indicates that shape anisotropy of nanowires is not strong enough to prevent occurrence of tip-induced magnetic field disturbance.

PACS numbers: 68.37.Rt, 62.23.Hj

1. Introduction

Prediction that some of the ZnO based diluted magnetic semiconductors (DMS) will exhibit room-temperature ferromagnetism caused the enhanced interest in these materials. Rapid thermal evaporation (RTE) enables one-dimensional ZnO growth with simultaneuos addition of a variety of elements. The final product of RTE process consists of different phases which may vary strongly in morphological form and composition. Although ferromagnetic ordering in Co-doped Y-shape ZnO nanostructures can be deduced from magnetization loops [1], the investigation requires relatively large material volume. To our knowledge there are no reports on nanometric-scale magnetic moments distribution in a given phase. The aim of our research was experimental verification of the presence of Co in a single ZnO nanowires (NWs). Magnetic force microscopy (MFM) which detects the existence of a magnetic moment with nanometric spatial resolution was used for this purpose. NWs with high shape anisotropy (i.e. high length to diameter ratio) are supposed to have magnetic moment which is detectable by MFM technique. It was shown in Ref. [2] that majority of electrodeposited Co nanowires with 30 nm diameter and lengths above 1 μm exhibits single domain state.

2. Experimental

$Zn_{1-x}Co_xO$ (nominal $x = 0.08$) tetrapodes with arms of nanometric diameter and micrometric length are grown from mixture of zinc and cobalt acetate by RTE at 915 ℃. The process takes place in an open horizontal quartz tube furnace. The reaction products are transported outside the reaction zone by air convection flow and deposit at the end of the tube, from where the proper phase can be separated. An ensemble of as-grown tetrapodes of various dimensions exhibits magnetic hysteresis with the coercive field of ≈ 150 Oe even at nearly room temperature (250 K), as revealed by SQUID measurements. The larger is the NW's shape anisotropy the higher is its contribution to the measured value of coercive field.

Two procedures were used to obtain single NWs deposited on a silicon surface. Here we report results obtained on well separated NWs deposited from methanol suspension. The second method (resulting in more dense distribution since the NWs attract to each other) was based on "dry" grinding the tetrapode powder onto a substrate and used only for verification of MFM contrast reliability. The suitable areas as large as tens $(\mu\text{m})^2$ which contain long, separate NWs were chosen by AFM or scanning electron microscopy (SEM) imaging prior to MFM measurement. MFM was performed in ambient air using Lift$^{\text{TM}}$ on MultiMode Nanoscope IIIa with non-magnetic scanner. The cantilever oscillation phase shift (in degrees, relative to the piezo drive) caused by vertical gradients in magnetic forces acting on a vibrating magnetic tip was used to produce MFM image. Standard magnetic etched silicon probe (MESP) tips having 10–150 nm Co/Cr magnetic coating with typical values of coercivity $\approx$ 400 Oe and magnetic moment of $\approx 10^{-13}$ emu were used. The ideal tip is an elongated

magnet (with its long axis perpendicular to the sample surface) which probes the sample with its bottom pole; MESP can be approximated by a magnetic monopole with charge $\delta = 10^{-8}$ A/m when placed 200 nm above a high coercivity sample [3]. For direct comparison all MFM results presented in this paper were obtained with the same tip and operated with the same drive and setpoint amplitude.

3. Results and discussion

Figure 1a shows AFM image of several single NWs having diameters of tens of nanometers (Fig. 1b) and lengths less than 1 μm. Figure 1c is a corresponding MFM image (lift height 25 nm, larger than NW diameter, therefore later referred to as "large" lift) which shows that each NW exhibits distinct MFM contrast recognizable as the area around the NW where the tip is attracted. Additionally, topography clearly appears in MFM, but for larger lifts the MFM signal becomes undetectable (it depends on a magnetic moment of a single NW and is quite low here, 0.2°, Fig. 1d). Instead of two opposite poles at the ends of a NW bar magnet (predicted for the case when the tip does not influence the sample) each NW is magnetized to be attracted to the tip (MFM tip strongly affects the sample in its vicinity).

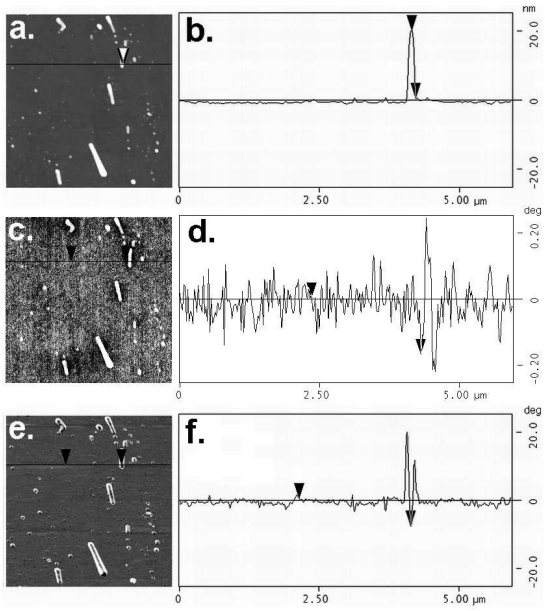

Fig. 1. (a) 6×6 μm^2 topography; (b) topography section line: markers indicate the NW diameter 20.0 nm vertically (horizontal distance of 140 nm is a sum of tip and NW diameter); (c) corresponding "large" lift MFM image (25 nm lift height > NW diameter 20 nm) — NWs are surrounded with areas of attractive force gradient; (d) MFM section: markers indicate contrast 0.2°; (e) corresponding "low" lift MFM image (20 nm lift height) — attractive force gradient along NWs axes; (f) MFM section: markers indicate contrast 8° (note the vertical scale is 100× magnified in comparison to (d)).

The maximum contrast (phase shift $\Delta\varphi$) obtained from a spherical particle (diameter d_p, magnetic moment $M_\mathrm{p}V_\mathrm{p}$) with a uniformly magnetized spherical tip (with effective magnetic moment $M_\mathrm{t}V_\mathrm{t}$, where M_t — remanent magnetization 1400 Oe/cm^3 of Co tip capping; V_t — effective volume in the order of 10^5 nm^3 of the interactive part of the tip)

$$\Delta\varphi_{\max}(h) = -\frac{2\pi^2 Q}{3k}\frac{M_\mathrm{p}\, d_\mathrm{p}^3\, M_\mathrm{t}\, d_\mathrm{t}^3}{h^5}$$

[4] (point probe approximation) strongly depends on the distance h between tip and sample (spring constant k and quality factor Q are parameters characterizing the cantilever). In our case instead of a spherical particle, a 1 μm long, 20 nm diameter NW of 10^6 nm^3 volume is imaged. Since the nominal Co content is 8%, the effective magnetic moment is lower than that of the tip. The NW's shape anisotropy is not large enough to produce coercive field larger than probe stray field, therefore the MFM contrast corresponds to out-of-plane magnetization disturbance and NW magnetization is fully oriented along the probe field. The contrast is not reversed (i.e. is always attractive) upon tip magnetization reversal which indicates reversible tip-induced perturbation in the sample, characteristic of soft magnetic materials and susceptibility mapping [5].

MFM contrast (its resolution and sensitivity) might be enhanced by decreasing tip–sample distance h, i.e. the lift height. Applying lower lift height (20 nm, which is comparable to NW diameter and therefore referred to as "low" lift) results in better signal-to-noise ratio (Fig. 1e) and a sensitivity improvement by 2 orders of magnitude (Fig. 1f compared to Fig. 1d). For "low" lift also the resolution is better (i.e. the area "seen" by the probe is smaller) and attractive regions are localized along NWs' axes. However in the case of low lift the topography strongly influences MFM. That is because when the tip apex is situated below the particle height (which occurs when the lift height is smaller than the particle height) a part of the tip may interact with sign opposite to that of the interactions originating from the rest of tip coating [6]. Thus inversing of the MFM contrast along NW borders occurs during imaging with "low" lifts.

To ensure that the measured contrast does not originate from impurities introduced by wet preparation method also "dry" (grinded) NWs were measured. The same MFM tip operated at the same drive and setpoint settings produced qualitatively comparable MFM images for both "large" and "low" lifts cases.

4. Conclusions

It was shown that RTE grown $Zn_{1-x}Co_xO$ NWs exhibit MFM contrast. Existence of magnetic moments is specific for the investigated NWs and does not originate from Co particles or Co-containig contaminants which could possibly be introduced during the preparation procedure. Nanometric spatial resolution of MFM does not allow to answer the question of how magnetic Co atoms

are distributed in NW volume. MFM enables only measuring magnetic structures at the level comparable to the magnetic moment of the tip (i.e. convolution of tip dimension, properties of magnetic coating and the distance between the tip and sample) and in our case only NWs' magnetic moments rearranged by the tip are detected. A resolution improvement is expected for longer NWs and magnetic probes with lower magnetic moment.

Acknowledgments

The research was partially supported by the European Union within European Regional Development Fund, through grant Innovative Economy (POIG.01.01.02-00--008/08) and by the MNiSW through grant No. N515 015 32/0997.

References

[1] X.M. Zhang, W. Mai, Y. Zhang, Y. Ding, Z.L. Wang, *Solid State Commun.* **147**, 293 (2009).

[2] J.M. Garcia, A. Thiaville, J. Miltat, *J. Magn. Magn. Mater.* **249**, 163 (2002).

[3] E.F. Wassermann, Ch. Burgel, A. Carl, J. Lohau, *J. Magn. Magn. Mater.* **239**, 220 (2002).

[4] V.L. Mironov, D.S. Nikitushkin, Ch. Binns, A.B. Shubin, P.A. Zhdan, *IEEE Trans. Magn.* **43**, 3961 (2007).

[5] V.L. Mironov, B.A. Gribkov, D.S. Nikitushkin, S.A. Gusev, S.V. Gaponov, A.B. Shubin, P.A. Zhdan, Ch. Binns, *IEEE Trans. Magn.* **44**, 2296 (2008).

[6] D.V. Ovchinnikov, A.A. Bukharev, *Proc. SPIE, Micro Nanoelectron.* **5401**, 642 (2003).